Elution-free hollow-fiber membranes of block copolymers for hemodialysis balancing protein retaining and toxin clearance

Xiang Ying [a], Shoutian Qiu [b,**], Xiangyue Ye [a], Zhuo Li [a], Jiemei Zhou [a], Yong Wang [a,*]

[a] State Key Laboratory of Materials-Oriented Chemical Engineering, College of Chemical Engineering, Nanjing Tech University, Nanjing, 211816, Jiangsu, China
[b] College of Materials Science and Engineering, State Key Laboratory of Materials-Oriented Chemical Engineering, Nanjing Tech University, Nanjing, 211816, Jiangsu, China

ARTICLE INFO

ABSTRACT

Hemodialysis has been used as the primary treatment for patients with end-stage renal disease, however, the current hemodialysis membranes still need complicated modifications to enhance the hemocompatibility and overcome the additive leaching issue. Herein, we prepare hemodialysis hollow-fiber membranes (HFMs) via the melt spinning and selective swelling of the block copolymers of polysulfone (PSF) and polyethylene glycol (PEG), PSF-*b*-PEG. PSF-*b*-PEG is first melt-extruded to form dense hollow fibers, and then soaked in selective solvents to transform the PEG microdomains into nanopores following the mechanism of selective swelling-induced pore generation, thus producing HFMs with three dimensionally interconnected porosities. As neither additives nor involatile solvents are involved in the manufacturing process of the HFMs, no elution of any organic matters could be detected for the HFMs during hemodialysis. The HFMs possess a symmetrical structure ensuring tight selectivity, and hydrophilic PEG chains are enriched on the pore surfaces, thus endowing the membranes with enhanced hydrophilicity and durable biocompatibility. We systematically investigate the effect of PEG contents and swelling conditions on pore sizes, porosities, surface properties, and consequently the hemodialysis performance. The optimized HFMs reject >99 % serum albumin while clear ~70 % middle molecular toxins such as lysozyme and 93–95 % small molecular toxins including urea, phosphate and creatinine. This work provides a strategy to prepare elution-free hemodialysis membranes by taking advantage of selective swelling of block copolymers to balance high protein retaining and high clearance of middle and small molecular toxins, and demonstrates their superiority in hemodialysis performance and safety than conventional membranes.

1. Introduction

Chronic kidney disease is a debilitating disease that patients suffer from an incapability of filtering blood by removing waste products from human body [1–3]. In general, while critical patients with renal failure or end-stage renal disease (ESRD) have to undergo kidney transplantation, most patients prefer to choose blood purification to relieve the suffering. Among all the therapies, hemodialysis is currently considered a highly successful treatment in functioning as the artificial kidney in the case of kidney failure [4,5]. The core component in the hemodialysis system is the dialyzer consisting of functional semi-permeable membranes, which selectively removes accumulated metabolic waste products and middle-molecular-weight protein toxins from blood while retains beneficial proteins for human body [6].

As hemodialysis membranes are on exposure to blood directly, it is highly demanded to ensure they have good biocompatibility especially on membrane surfaces [7]. Hemodialysis membranes can be prepared by various synthetic polymers such as polymethylmethacrylate (PMMA) [8], polyvinylidenefluoride (PVDF) [9], polyethersulfone (PES) [10,11] and polysulfone (PSF) [12–14]. However, most of these membrane-forming polymers are hydrophobic, which usually lack biocompatibility and may cause serious risks to patients [15]. For example, the adsorption of proteins during hemodialysis may lead to serious life-threatening complications as a result of the activation of complement replacement pathway [16]. One strategy to improve the biocompatibility is grafting hydrophilic agents or coating additives (such as heparin) onto membrane surfaces [17–19]. However, these grafting or coating procedures are usually complicated and costly. Some

---

researchers choose to blend hydrophilic additives, such as poly-vinylpyrrolidone (PVP) and polyethylene glycol (PEG), directly in the membrane-forming materials for the sake of economic benefits and scale production [20–23]. Nevertheless, these hydrophilic additives are highly soluble in water, which are very likely to leach out during the membrane preparation process [24]. Moreover, the shear force between membrane surface and the circulating fluid may also lead to the scouring of additives on membrane surfaces during dialysis, thus resulting in a potential hazard to cause kidney complications [15]. Therefore, it is highly demanded to develop membranes with little or zero elution of additives and any other organic components from the membranes.

In recent years, amphiphilic block copolymers (BCPs) are adapted to avoid the leakage of additives as polymer chains of different blocks are joined by covalent bonds [25,26]. Researchers blended triblock poly (vinyl pyrrolidone)-*b*-poly (methyl methacrylate)-*b*-poly (vinyl pyrroli-done) and comb-like amphiphilic poly (vinyl pyrrolidone)-*block*-poly (acrylate)-*graft*-poly (methyl methacrylate)-*block*-poly-(vinyl pyrroli-done) (PVP-*b*-P(AE-*g*-PMMA)-*b*-PVP) with the PES homopolymer, which was the base membrane-forming polymer, to prepare hemodialysis membranes. The leaching-out of hydrophilic components was therefore reduced during hemodialysis due to the presence of PMMA or P (AE-*g*-PMMA) chains entangled with the chains of the PES base polymer [27,28]. In addition , Zhong et al. [29] used BCPs as the only raw material to prepare flat-sheet membranes by the process of nonsolvent induced phase separation (NIPS) without the involvement of any additives. Thus-prepared hemodialysis membranes showed excellent hemo-compatibility and biocompatibility. However, all these hemodialysis membranes discussed above were prepared by NIPS. On one hand, they exhibited relatively wide pore size distributions, which functioned inefficiently in removing middle molecular toxins (β2-microglobulin, myohemoglobin, *etc.*) with the risk of albumin loss [30]. On the other hand, organic solvents with high boiling points including *N*, *N*-dime-thylacetamide (DMAc) and *N*-methyl pyrrolidone (NMP) are inevitably used during NIPS. These solvents are hard to be completely removed from the formed membranes and may leach out during the dialysis process. Therefore, hemodialysis membranes with no elution of organics and more precise separation performance, especially the clearance of middle molecular toxins, are highly desired.

Very recently, we reported the preparation of HFMs by the melt spinning and selective swelling of polysulfone-*block*-poly(ethylene gly-col) (PSF-*b*-PEG), which neither uses any organic solvents nor produces wastewater [31]. Thus-prepared membranes displayed symmetrical structures, uniformly dispersed pore sizes as well as high porosities, thus exhibiting promising ultrafiltration (UF) performance. However, this strategy has not been used to prepare membranes for biomedical ap-plications, especially hemodialysis membranes where excellent selec-tivity, biocompatibility and safety are required. In this work, we report the preparation of HFMs via the melt spinning and selective swelling of PSF-*b*-PEG with varied PEG contents, and demonstrate the feasibility of the PSF-*b*-PEG HFMs as hemodialysis membranes. As-prepared HFMs show high removal of small solutes and middle molecular protein toxins on the premise of little or no loss of beneficial macromolecular proteins (Scheme 1). Importantly, nearly zero elution of organics could be found for PSF-*b*-PEG HFMs because PEG is covalently linked to PSF matrix and no high boiling solvents are involved in the membrane-manufacturing process.

2. Experimental section

2.1. Materials

PSF-*b*-PEG block copolymers with varied PEG contents were ob-tained from Nanjing Bangding. The PEG percentage of three BCPs were 21, 30, and 40 wt%, respectively (Fig. S1). Herein, they are named as SFEG21, SFEG30, and SFEG40. According to the manufacturer, the co-polymers were synthesized by the transetherification reaction, and they are linear block copolymers; the number-average molecular weight of the PEG block is ~20 kDa while the number-average molecular weight of PSF blocks for SFEG21, SFEG30, and SFEG40 were 60.1, 44.7, 33.2 kDa. Urea (60.06 Da, ≥98 %) was purchased from Aladdin. Sodium chloride (NaCl, ≥99.5 %) was obtained from Xilong Scientific, LDC. Lysozyme from egg white (14–15 kDa, 40000 U/mg), sodium dihy-drogen phosphate (NaH$_2$PO$_4$·2H$_2$O, ≥99.0 %) and vitamin B12 (VB-12, 1.35 kDa, ≥98 %) were supplied by Macklin. *n*-propanol (Extra Dry, 99 %) was purchased from Energy Chemical. Bovine serum albumin (BSA, 66 kDa, >97 %) and myohemoglobin (Mb, 16.7 kDa, ≥95 %) were ob-tained from Sigma-Aldrich. Creatinine (113 Da, ≥99 %) and phosphate buffer solution (PBS) tablets were supplied by MP Biomedicals, LLC. Acetone (≥99 %) was purchased from Sinopharm. Platelet-rich plasma (PRP) solutions and whole pig blood were provided by Shanghai yuanye Bio-Technology Co., Ltd. The reagent kits of activated partial throm-boplastin time (APTT), prothrombin time (PT), thrombin time (TT), fibrinogen (FIB) and clotting factor deficient plasma were obtained from Simens. All chemicals were used without further purifications.
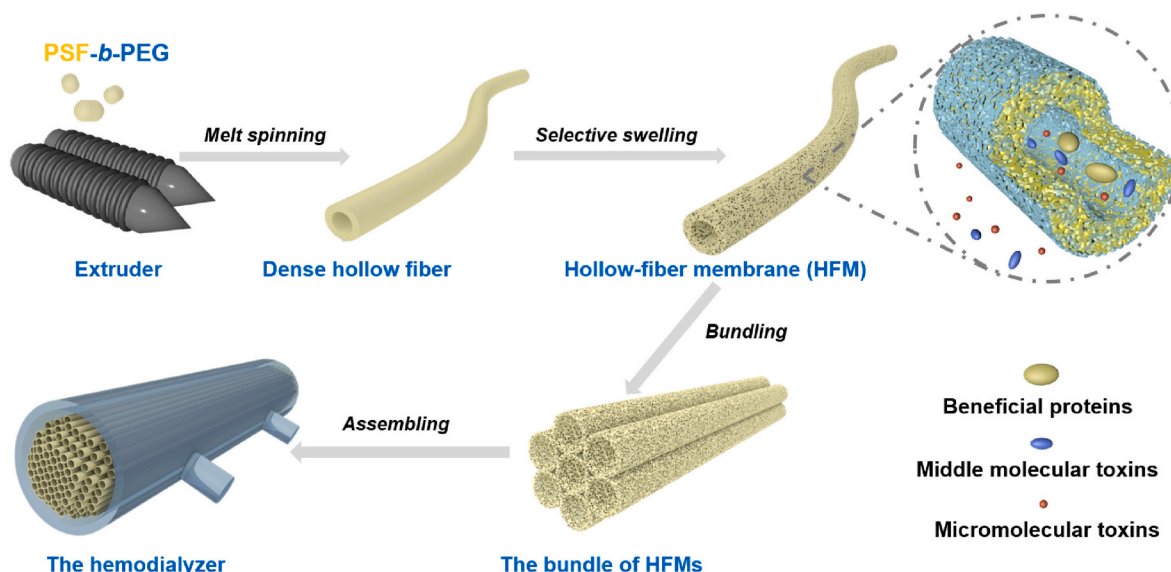
Scheme 1. Scheme for the preparation of a hemodialyzer using HFMs prepared by melt spinning of PSF-*b*-PEG followed by selective swelling.

Deionized (DI) water was homemade and used throughout this work.

2.2. Preparation of PSF-b-PEG hollow-fiber membranes

Primary PSF-*b*-PEG hollow fibers (HFs) were extruded via a micro twin-screw extruder (with a heating spinneret, Xinshuo, WLG10G). The extruder is composed of two chambers up and down while the temperature of the lower cavity is always higher than that of the upper cavity. The melt-spun temperature for SFEG21, SFEG30, and SFEG40 were set as 180/190 °C, 175/185 °C, and 160/170 °C, respectively. During selective swelling, primary hollow fibers were immersed directly in the swelling solvent (a mixed solvent including 80 wt% *n*-propanol and 20 wt% acetone) at preset temperatures (ranged among 55–70 °C) for certain durations (0.5–3 h) to generate interconnected nanopores [31]. After being withdrawn from the selective solvent, the HFMs were then dried at 40 °C for at least 4 h to evaporate all residue solvents.

2.3. Characterizations

The cross-sectional and surface morphologies of PSF-*b*-PEG HFMs were observed using the field-emission scanning electron microscopy (SEM, Hitachi S4800). Before imaging, an ultrathin layer of gold was sputtered on the sample surface to enhance the conductivity. The cross sections of HFMs were prepared by fracturing in liquid nitrogen. The surface porosity and the pore size distribution were estimated by calculated the pore numbers on the surface SEM images with the software of *ImageJ* and *Nano Measure*, respectively. The water contact angles (WCAs) of SFEG30 hollow fibers and HFMs were measured on a contact angle goniometer (Dataphysics DCAT21). During test, water was dropped on the outer surface of SFEG30 hollow fibers and HFMs. Each sample was tested at least 5 times to take the average value. Zeta potential was tested using an electrokinetic analyzer (SurPASS, Anton Paar). During test, the electrolyte environment was simulated using a 1.0 mmol L^{-1} potassium chloride (KCl) aqueous solution.

2.4. Filtration tests

PSF-*b*-PEG HFMs were installed in the pressure permeation test device, followed by pre-pressing with DI water for 30 min under a 1500 mmHg transmembrane pressure. During test, the pressure was set as 375 mmHg firstly, and then gradually raised to 750, 1125 and 1500 mmHg, respectively to measure the infiltration water volume within 30 min under each pressure. The relations between the acquired flux and transmembrane pressure were calculated. The average of the results indicates the UF coefficient (mL h^{-1} m^{-2} mmHg^{-1}) of PSF-*b*-PEG HFMs.

The molecular weight cutoff (MWCO, the molecular weight of 90 % rejection of dextran) of PSF-*b*-PEG HFMs was tested using a mixed dextran solution in the pressure permeation test device. 2.5, 1, 1, and 2 g dextran with different molecule weight (10, 40, 70 and 500 kDa) were added into 1 L DI water to prepare the mixed dextran solution was prepared. Dextran concentrations were tested using a gel permeation chromatography (GPC, Waters 1515), and the effective pore sizes of HFMs were determined by Eq. (1) [32,33]:

$$r = 0.33 \, Mw^{0.46} \tag{1}$$

where *r* (Å) represents the effective pore size of PSF-*b*-PEG HFMs while *Mw* (Da) is the MWCO of dextran.

2.5. Performance assay

To evaluate the hemodialysis performance of HFMs, a homemade apparatus was manufactured. The schematic diagram of the device to simulate the hemodialysis process is shown in Fig. S2. A lab-scale hemodialyzer was prepared by sealing a bunch of HFMs in a PMMA pipe (15.0 × 9.3 cm^3). Both ends of the pipe were potted with the

Lantian 9005 epoxy and polyurethane adhesives. The total effective area of HFMs in the lab-scale hemodialyzer was set as 0.15 m^2 by equipping varied numbers of HFMs. The prepared modules were equilibrated in DI water overnight prior to the test.

In the performance assay, several simulated solutions were used as simulated blood during hemodialysis. The 1.0 g L^{-1} BSA solution was prepared by adding 0.5 g BSA into the 500 mL PBS solution to simulate the human serum albumin in blood. 0.2 g L^{-1} lysozyme, myoglobin and Vitamin B12 (VB-12) solutions were formed by adding 0.1 g lysozyme, myoglobin and VB-12 into 500 mL PBS solutions as representatives of the middle molecular toxins in blood. 1.5 g urea and creatinine (on behalf of the small solutes) were added to the 500 mL PBS solution to form the 3.0 g L^{-1} urea and creatinine solution, respectively. Herein, the PBS solution was also used as the simulated dialysate as a contrast.

2.5.1. BSA rejection

The PBS solution was pre-dialyzed for 30 min prior to dialysis and replaced with the BSA solution when the test solution was stable. During dialysis, the simulated blood passed from the inner surface of HFMs at 100 ml min^{-1} while the simulated dialysate passed from the outer surface of HFMs 300 ml min^{-1}. The dialysis test lasted for 4 h, then the absorption peak of BSA at 280 nm was measured using a UV spectrophotometer. The rejection to BSA (*R*, %) is calculated according to Eq. (2):

$$R \, (\%) = \left(1 - \frac{C_{Bo}}{C_B}\right) \times 100\% \tag{2}$$

where C_{Bo} represents the initial concentration of the BSA solution while C_B is the BSA concentration after dialysis.

2.5.2. Toxin clearance assay

The PBS solution was pre-dialyzed for 30 min prior to dialysis and replaced with the BSA solution when the test solution was stable. The dialysis procedure is the same as the BSA rejection. After an 4 h dialysis test, the absorption peaks of Lysozyme (280 nm), myoglobin (405 nm), VB-12 (552 nm), urea (420 nm), and creatinine (230 nm) were measured using a UV spectrophotometer. The clearance rate of toxin is calculated according to the following Eq. (3):

$$Clearance \, (\%) = \left(1 - \frac{C_{To}}{C_T}\right) \times 100\% \tag{3}$$

where C_{To} represents the initial concentration of simulated blood while C_T is the concentration after dialysis.

2.5.3. Phosphate clearance assay

A 1.0 g L^{-1} phosphate solution was prepared by adding 1.0 g phosphate to the 500 mL PBS solution and was used as the simulated blood. The PBS solution was used as the simulated dialysate. Phosphate concentration was measured by phosphorus-molybdenum blue colorimetry. The calculation equation is the same as Eq. (3).

2.6. Hemocompatibility assay

2.6.1. Protein adsorption

Both the 3 cm-length SFEG30 hollow fibers and HFMs were immersed in the 1.0 g L^{-1} BSA solution and incubated at 30 °C for 12 h. In the experiments, BSA was dissolved in PBS at a concentration of 1.0 g L^{-1}. The pH of BSA solution was measured by a conductivity meter (S230–K, Mettler Toledo). The samples were gently shaken to reach equilibrium between adsorption and desorption of proteins. The concentration of BSA before and after test was measured using the UV spectrophotometer at 280 nm to calculate the number of proteins adsorbed on membrane surfaces. All samples were tested at least three times to obtain a mean value.

2.6.2. Static platelet adhesion

Both the 3 cm-length SFEG30 hollow fibers and HFMs were firstly placed in separate 24-well cell culture plates containing PBS buffer and incubated at 37 °C for 1 h. During test, the samples were incubated in fresh porcine platelet-rich plasma (PRP) at 37 °C for 2 h. Then, the PRP was removed and each well was rinsed 3 times with the PBS solution. 2.0 ml 2.5 wt% glutaraldehyde was then added to each well, followed by incubating at 4 °C for 1 h. Afterward, the samples were dehydrated with different concentrations of mixed solutions of ethanol and water (2:8, 4:6, 6:4, 8:2 and 10:0; each for 10 min) and then dried at room temperature overnight. Platelet count and morphology were observed by SEM.

2.6.3. Hemolysis

Both the 3 cm-length SFEG30 hollow fibers and HFMs were immersed in saline solution at 37 °C for 40 min, and commercial membranes (named as A, B, and C) were also tested for comparison. Subsequently, 200 μL pig blood was added to the saline and incubated at 37 °C for 1 h. DI water was used as the positive control group while the saline was used as the negative control group. After centrifuged at 3000 rpm for 10 min, the absorption peak of the supernatant at 545 nm was measured by UV spectrophotometer. The hemolysis rate (*HR*) is calculated by the following Eq. (4):

$$HR\ (\%) = \frac{As - An}{Ap - An} \times 100\% \tag{4}$$

where A_n and A_P are the absorption peak of the negative and positive control groups, respectively. A_S represents the absorption peak of the supernatant.

2.6.4. Clotting time tests

Both the 3 cm-length SFEG30 hollow fibers and HFMs were placed in 1.5 mL centrifuge tubes and incubated with 1.0 mL of platelet-poor plasma (PPP) at 37 °C for 30 min, 1 mL PPP was added to a 1.5 mL blank centrifuge tube as a blank control. The sample and blank groups were each repeated 3 times. After incubation, 500 μL PPP samples were taken from the sample set and blank tubes, added to activated partial thromboplastin time (APTT), prothrombin time (PT), thrombin time (TT) and fibrinogen (FIB) matching reagents (Siemens Germany, batch number 10446923). The APTT, PT, TT and FIB values were determined using a fully automated coagulation analyzer (CS-5100, SYSMEX).

2.7. Elution evaluation of organics

The leaching-out of PEG was tested by comparing the peak intensities of PEG in water before and after dialysis. DI water and a 0.1 g L^{-1} PEG aqueous solution were configured as blank control. The PEG content of samples was measured by gel permeation chromatography (GPC, Waters 1515).

The amount of total organic carbon (TOC) of SFEG30 HFMs and the PEG solution were tested using a total organic carbon analyzer (multi N/C 3100). SFEG30 HFMs were dialyzed in DI water for 4h using the dialysis device (Fig. S2b). 20 ml DI water was also tested as blank control. Each set of samples was tested three times to obtain an average value.

3. Results and discussion

3.1. Selective swelling of PSF-b-PEG HFMs

In hemodialysis, the removal of solutes (e.g., urea, creatinine, phosphate, VB12 and β2-microglobulin) occurs through a combination effect of diffusion, convection and adsorption and is governed by the membrane properties including pore size, wall thickness and surface area [34]. Although PSF-*b*-PEG HFMs exhibit tunable pore sizes and porosities depending on the swelling conditions (swelling temperature and swelling time) [35], they were only used in the rejection to proteins with relatively high molecular weights such as BSA, while their rejections to middle molecular proteins remain unexplored. Herein, we investigated the relationship between pore characteristics and hemodialysis performance of PSF-*b*-PEG HFMs with varied PEG contents. As shown in Fig. 1a–c, all PSF-*b*-PEG HFMs prepared in this work exhibited a symmetrical structure along the sections with the pore sizes in the scale of several tens of nanometers. Such a symmetrical structure is in stark contrast to the asymmetric structure in membranes prepared by NIPS, which is composed of a support layer with large pores and a selective layer with smaller pores [31].

It is also clearly shown that the swelling behaviors depend heavily on the composition of PSF-*b*-PEG. The swelling degree of PSF-*b*-PEG HFMs is enhanced with the increased PEG contents. Herein, we tested their MWCOs to estimate the effective pore sizes of the PSF-*b*-PEG HFMs. The average pore sizes of the SFEG21 HFMs and SFEG30 HFMs were thereby estimated to be approximately 8.8 nm and 14.7 nm, respectively (Figs. S4a and b). The pores of the SFEG21 HFMs and SFEG30 HFMs were also estimated to be 7.8 nm, 13.3 nm, respectively, by SEM observations. The pore sizes of SFEG21 and 30 HFMs were smaller or close to the major axis of BSA (molecular size: 14.1 nm × 4.2 nm x 4.2 nm) [36,37]. Also considering the entire wall serves as the selective layer, we can understand that all the HFMs show high rejection to BSA. SFEG21 HFMs showed relatively small pore size on the membrane surface (~8.8 nm). The size was much larger than that of lysozyme having a roughly elliptical shape (1.9 nm × 2.5 nm × 4.3 nm) [38]. However, as the thickness of the effective separation layer was about tens of microns, SFEG21 HFMs were less penetrative to middle molecular proteins. As shown in Fig. 1d, the clearance of lysozyme and myoglobin was only 34.2 % and 22.2 %, respectively. For SFEG30 HFMs, the larger pore size (14.7 nm) and the narrow pore distribution (Fig. S5) ensured the high clearance of middle molecular protein toxins (69.2 % for lysozyme and 49.8 % for myoglobin). When the PEG content was increased to 40 %, the membrane showed a relatively low porosity as a result of the excessive swelling while the membrane surface was almost clogged by the continuously migrated PEG chains [39]. Thus, SFEG40 HFMs showed the lowest clearance of middle molecular toxins (4.2 % for lysozyme and 2.0 % for myoglobin). Therefore, the rejection performance of PSF-*b*-PEG HFMs with varied compositions depended primarily on the varied membrane pore size determined by the process of selective swelling.

We then studied the performance of SFEG30 HFMs swelled at different swelling temperatures and durations. It is found that the swelling degree of PSF-*b*-PEG HFMs increased with rising swelling temperature and time while excessive swelling degree was achieved under elevated swelling temperatures and prolonged swelling time. Typically, lower swelling degree resulted in low clearance of middle molecular toxins, and excessive swelling degree led to abnormal permeation processes. More detailed results and discussions were given in **SI**. Thus, we identified effects of the PEG content, swelling time and temperature on the rejection performance of PSF-*b*-PEG HFMs and obtained the optimized HFMs. The SFEG30 HFMs prepared by swelling at 65 °C for 1 h exhibited the best overall performance (>99 % rejection to BSA, as well as high clearance of 69.2 % for lysozyme and 49.8 % for myoglobin) and are the best candidate for hemodialysis. Therefore, we used the SFEG30 HFMs prepared under this condition to assemble hemodialyzers, which are subjected to extensive studies in subsequent studies.

3.2. Hemodialysis performance of SFEG30 HFMs

Hemodialysis membranes are used for the removal of toxins from blood and thus demand high permeability and precise separation performance. The hemodialysis performance of SFEG30 HFMs were shown in Fig. 2. Thanks to the high porosity and symmetry of the membrane,
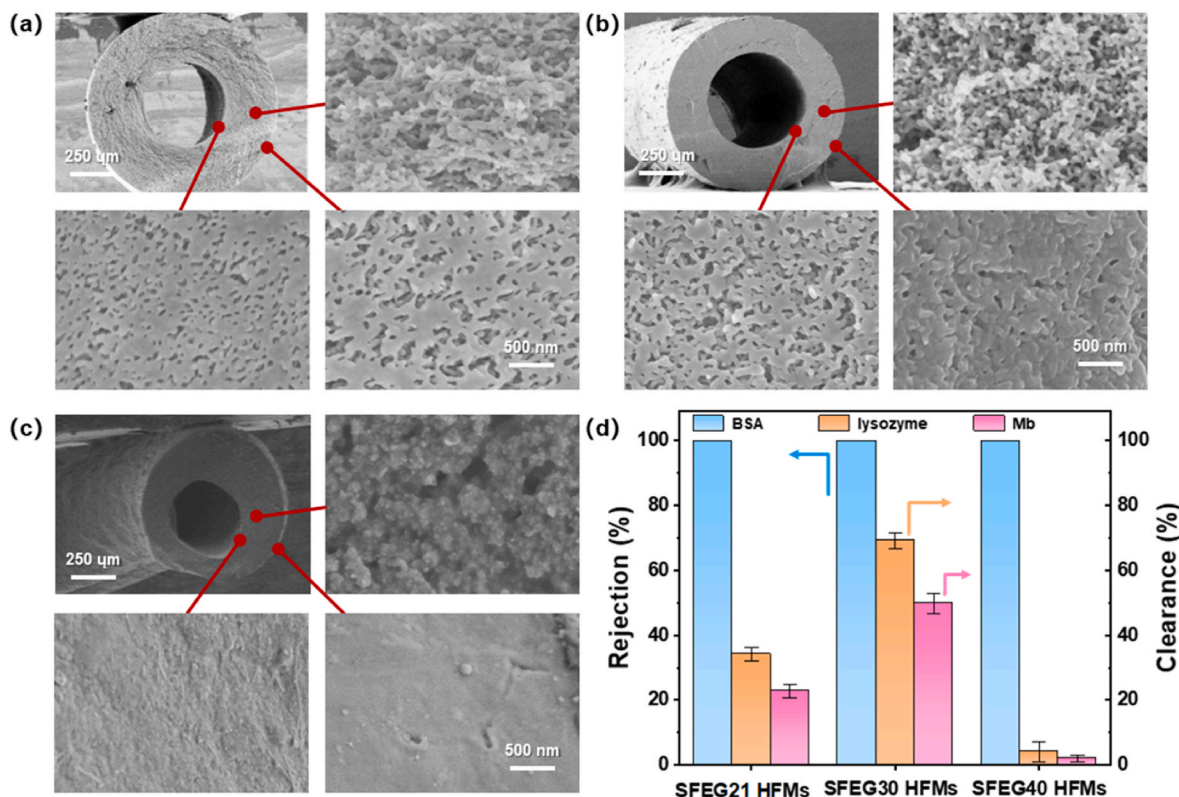
Fig. 1. Cross-sectional pictures, inner surface, outer surface and cross-sectional SEM images of the (a) SFEG21 HFM, (b)SFEG30 HFM, and (c) SFEG 40HFM prepared by swelling at 65 °C for 1 h; (d) the rejection to BSA and the clearance of lysozyme and Mb for the SFEG21 HFMs, SFEG30 HFMs, and SFEG40 HFMs.
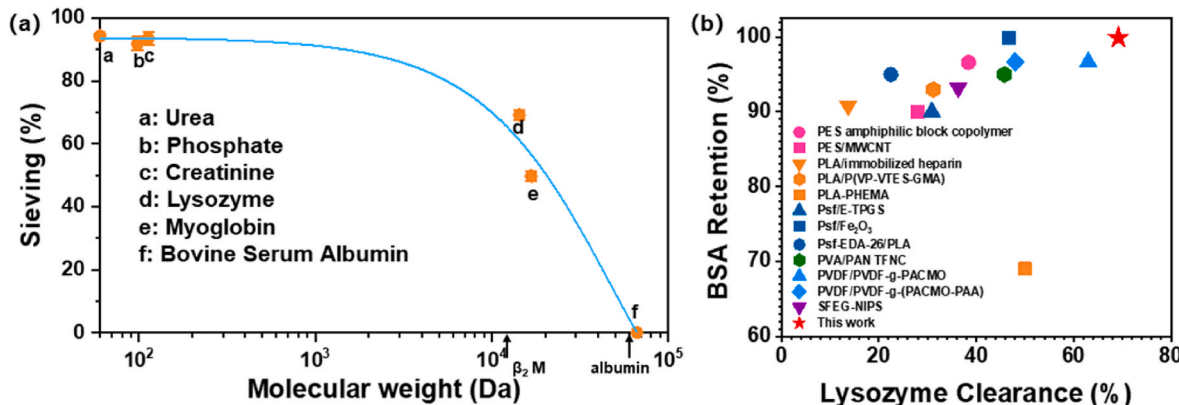

Fig. 2. (a) Sieving coefficient of SFEG30 HFMs for solutes with different molecular weights. (b) Performance comparison of different hemodialysis membranes.

SFEG30 HFMs had a UF coefficient of 25.4 mL h^{-1} m^{-2} mmHg^{-1} (measured in the transmembrane pressure range of 375–1500 mmHg) and could be classified as a high-flux hemodialysis membrane [40]. Typically, SFEG30 HFMs exhibited a high rejection to BSA (~99.9 %). As the molecular weight of BSA (66 kDa) is similar to that of Human Serum Albumin (HSA) (67 kDa), we concluded that SFEG30 HFMs can retain almost all the beneficial human proteins during hemodialysis.

Moreover, SFEG30 HFMs also displayed high removal of small molecular toxins (the diffusive solute) because the clearance mechanism is mainly attributed to the dispersion effect. As shown in Fig. 2a, the clearance rates of small molecular toxins such as urea, phosphate and creatinine were relatively stable and maintained among 93–95 %. The reason of high clearance rate of small molecular toxins may be ascribed to the relatively large pores and high porosity of SFEG30 HFMs which endow the membranes with high permeability and strong dispersion

effect during dialysis.

More importantly, high clearance of middle molecular toxins was also achieved for SFEG30 HFMs. β2-microglobulin is a representative of middle molecular toxins. The residue of β2-microglobulin in human body causes dialysis-associated amyloidosis. As the molecule weight of lysozyme (14–15 kDa) is slightly larger than that of β2-microglobulin (11.8 kDa), the clearance of lysozyme reflects that of β2-microglobulin. The clearance rate of lysozyme was as high as 69.2 %. This is reasonable because the average pore size of the membrane was estimated to be approximately 14.7 nm (Fig. S5b). As is illustrated in Fig. 2b, SFEG30 HFMs showed better comprehensive performances compared to membranes produced by other methods, especially in terms of the rejection to BSA and the clearance of lysozyme. In addition, SFEG30 HFMs also achieved a clearance up to 49.8 % for myoglobin, which is close to the clearance of commercial membranes. The high clearance of middle

molecular toxins during dialysis allows for efficient dialysis treatment for patients.

3.3. Hemocompatibility of SFEG30 HFMs

3.3.1. Protein adsorption

Generally, plasma proteins will attach to the material when blood comes into contact with membrane surfaces, which usually causes platelet attachment and activation of the clotting phenomenon. The dynamic adsorption test of proteins for the SFEG30 hollow fibers before swelling treatment and HFMs was carried out using the 1.0 g L^{-1} BSA solution. As shown in Fig. 3b, the protein adsorption of SFEG30 was only 107 μg cm^{-2} while that of the dense hollow fiber before swelling was as high as 1507 μg cm^{-2}. Thus, selective swelling endowed the membrane with better adsorption resistance of proteins, which can be explained as follow: Firstly, proteins are more likely to adhere to hydrophobic materials, especially in aqueous systems. During the protein adsorption process, hydrated protein molecules displace water molecules on membrane surfaces through electrostatic interactions, thus reaching the thermodynamic equilibrium [41]. Therefore, membranes with hydrophilic surfaces are likely to show better adsorption resistance for proteins because water molecules on membrane surfaces are difficult to be replaced. As shown in Fig. 3a, the WCA of SFEG30 HFMs after swelling was decreased to 60° while that of the pristine hollow fiber was 72°, implying the enhanced hydrophilicity of SFEG30 HFMs after swelling. Such a decrease in WCA was also reported in PSF-*b*-PEG flat membranes, and this was mainly attributed to the enrichment of hydrophilic PEG chains on membrane surfaces after swelling [42]. PEG was abundant in ether bonds which was more conducive to tightly bound to water molecules via hydrogen bonds, thus forming a hydrated layer on membrane surfaces. Typically, the hydration layer acted as an energetic and physical barrier which could effectively prevent the adsorption of biological components to the membrane surface. The hydrophilic surface of SFEG30 HFMs promoted the anti-adsorption of proteins to a great extent. Besides, the charge on membrane surfaces should also be considered. Typically, the surface of most blood cells and blood vessel walls are negatively charged and may have static attraction with positively charged materials [43]. Therefore, a neutral or negatively charged surface facilitates blood compatibility. As can be seen from the zeta potential results in Fig. 3c, both the SFEG30 hollow fibers and HFMs were negatively charged. This is easily acknowledged because PSF has strong electronegativity and is predominantly distributed on the surface of the SFEG30 hollow fibers as ~70 wt% of the SFEG30 is PSF blocks. After swelling, the negatively charged nature of the HFMs is significantly weakened due to the enrichment of the PEG chain segments on the membrane surface, which makes the HFMs somewhat resistant to protein adsorption. The pH of the BSA solution was 8.55 in the adsorption experiment, which was higher than the isoelectric point of BSA protein (4.5) [37]. Therefore, BSA in this solution is negatively charged, and is hard to adsorb on the membrane surface which is also negatively charged.

3.3.2. Static platelet adhesion

Despite platelets play a positive role in hemostasis, they may lead to thrombosis when accumulating in blood [44]. Typically, platelets tend to accumulate on membranes with hydrophobic surfaces, such as polylactide (PLA) and PSF membranes [45]. To better understand the platelet adhesion of SFEG HFMs prepared by selective swelling, the adsorption behaviors of platelets on SFEG30 HFMs and hollow fibers were studied using SEM. As shown in Fig. 4a, b, a large number of platelets and erythrocytes were aggregated on the surface of SFEG30 hollow fibers. The erythrocytes were bound to each other and the aggregated platelets were in a reticular pseudopod structure, indicating that platelets adsorbed on the surface of the membrane had been activated. This is hazardous because platelet adhesion and activation are considered crucial issues leading to thrombosis and coagulation [46]. In contrast, only a few adsorbed platelets and individual erythrocytes could be seen on the surface of SFEG30 HFMs (Fig. 4c and d). According to the protein resistance test above, platelet adhesion and activation are related to the characters of the membrane surface, *i.e.*, the negatively charged membrane surface and hydrated layer formed by hydrogen bonds of PEG can effectively inhibit the adsorption behavior of platelets on the membrane surface.

3.3.3. Hemolysis

Generally, blood flows continuously through the dialysis membrane during hemodialysis when the blood-contacting material has good hemocompatibility. However, the risks of the release of hemoglobin rise with the rupture of erythrocytes as a result of the interaction between the red blood cells and hydrophobic membranes, which is called the hemolysis process. Typically, the extent of damage to red blood cells by the dialysis membrane is evaluated using hemolysis ratio (HR). The dialysis membrane is deemed harmless to humans when the HR value is lower than 5 % by the ASTM F756-2017 standard. To be more specific, it is classified into partial hemolytic when HR is 5%–2% and non-hemolytic when HR is lower than 2 %. As is shown in Fig. 5a, the results showed that the HR value of the SFEG30 hollow fiber was 4.4 %, which fits into the partial hemolytic. After swelling, the HR value of SFEG30 HFMs is dramatically decreased to 0.02 %, indicating that the PEG enriched on membrane surfaces can effectively inhibit the release of hemoglobin from cells. Therefore, the HFMs was typically a nonhemolytic membrane, and the HR value was much lower than the PSF-*b*-PEG flat membrane prepared by NIPS (with an HR value of 0.48 %) [29]. We also conducted a contrast experiment with three commercial membranes (Membrane A, B, and C are sampled from commercially available HFMs and assembled like SFEG30 HFMs). It is noticeable that the anti-hemolytic activation performance of SFEG30 HFMs were also superior to those of commercial membranes.
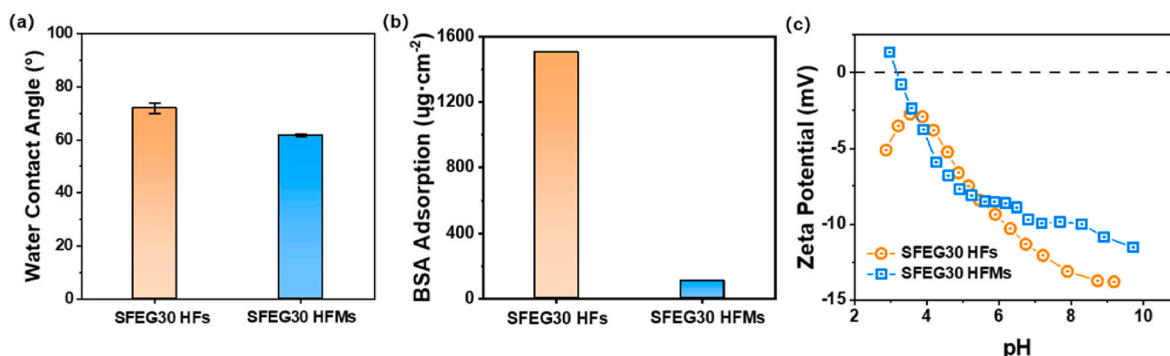

Fig. 3. (a) WCAs, (b) BSA adsorptions, and (c) Zeta potentials of SFEG30 hollow fibers and HFMs.
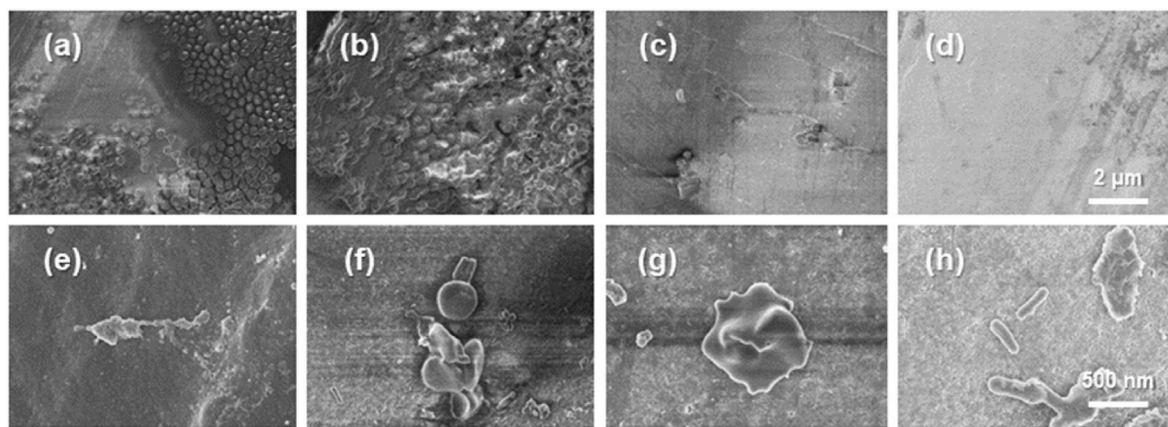
Fig. 4. SEM images of the platelet and erythrocyte gathered on the (a, b) outer and (e, f) inner surface of the SFEG30 hollow fiber, and the (c, d) outer and (g, h) inner surface of the SFEG30 HFM. Image (a–d) and (e–h) have the same magnification, and the scale bar is shown in d and h, respectively.
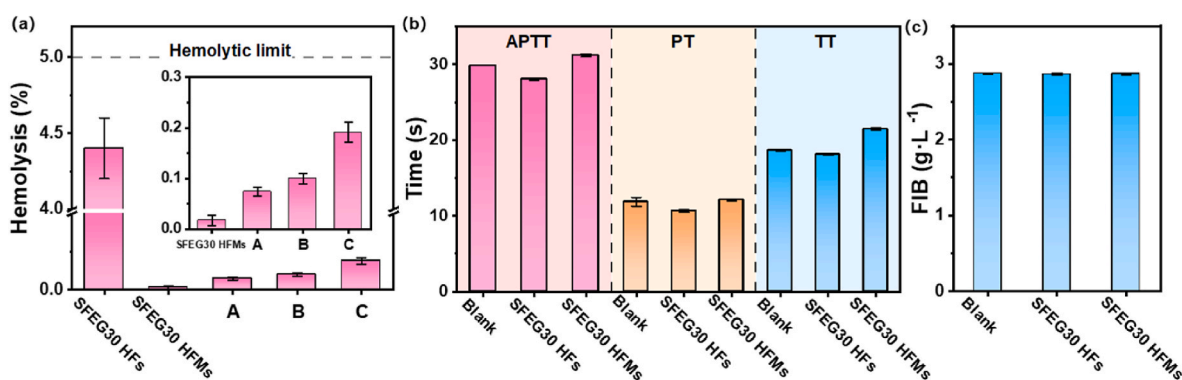

Fig. 5. (a) Hemolysis performance of SFEG30 hollow fibers, SFEG30 HFMs, and commercial membrane A, B, C. (b) Clotting time and (c) FIB adsorption test of SFEG30 hollow fibers and SFEG30 HFMs.

3.3.4. Clotting time

The coagulation time (including thromboplastin time (APTT), prothrombin time (PT) and thrombin time (TT)) of SFEG30 HFMs were measured. As shown in Fig. 5b, the APTT and PT values of the SFEG30 hollow fiber were 28.1 s and 10.6 s, while those of SFEG30 HFMs were 31.2 s and 12.1 s, respectively. Both the APTT and PT of platelet-poor plasma (PPP) of SFEG30 HFMs were slightly increased compared to the blank control. The blood coagulation cascade is used to examining intrinsic pathway, common pathway and extrinsic pathway, while APTT and PT only include the former two. To be more specific, APTT represents the time that coagulation is initiated by activator XII when blood contacts with the membrane surface, while PT is the time that coagulation begins with the addition of tissue factors and calcium ions. Typically, PT can only be prolonged by active substances such as heparin but not be prolonged by the substance itself. Therefore, the slight prolongation of ATPP and TT may be attributed to the improved hydrophilicity because of the migration and enrichment of PEG segments on surfaces of HFMs. The presence of PEG chains resulted in stronger interactions with antithrombin and thereby the prolongation of the action time. The mechanism is not identical to that of heparin, *i.e.*, the less PEG contact activation allows for a longer clotting time of the swelling-treated membrane. fibrinogen (FIB) and TT reflect the fibrinogen content and the time to convert to fibrin. As shown in Fig. 5b and c, TT exhibited the same results as APTT and PT, but there was a slight decline in FIB concentration after PPP treatment, indicating that both could absorb small amounts of FIB from plasma and had an effect on coagulation cascade events, but to a very low degree and do not affect normal physiological coagulation cascade events. Thus, SFEG30 HFMs does have good hemocompatibility, but moderate anticoagulant effect. This

may be explained as follow: first, the anticoagulant effect of PEG is very limited compared with other anticoagulants such as heparin. Second, the anticoagulant process is related to the molecular weight and total charge of PEG on the membrane surface [47].

3.4. Organic elution of SFEG30 HFMs

As the hydrophilic PEG-like additives easily leach out during hemodialysis, the gel permeation chromatography (GPC) was used to detect the content of PEG in the eluate in the simulated dialysis process. As can be seen from Fig. 6a, the PEG solution showed a clear peak at 30 min while there was no clear peak observed in both pure water and the water sample after dialysis, proving that there was essentially no PEG dissolution before and after dialysis. Typically, only PSF-*b*-PEG BCPs were used during the production of HFMs while PEG and PSF segments in PSF-*b*-PEG are tightly linked by covalent bonds. Furthermore, both melt-spinning at high temperature and the selective swelling in selective solvents did not corrupt the structure of BCPs. Therefore, no organic moieties from the membrane-forming copolymer, SFEG, could leach out during dialysis. Also, we further demonstrated that the melt-spinning and selective swelling method is non-destructive, *i.e.*, no chemical changes or mass loss are involved in the pore formation process.

Apart from hydrophilic solutes, other organics may dissolve into blood during hemodialysis. Therefore, the elution of other organics was also characterized by measuring the TOC in an aqueous solution after dialysis. As shown in Fig. 6b, the TOC value was very high (13840 μg L^{-1}) when organic matters were dissolved in an aqueous solution (0.1 g L^{-1} PEG solution was used as an example). However, almost no organic matters increase (<50 μg L^{-1}) could be detected as the TOC in the liquid
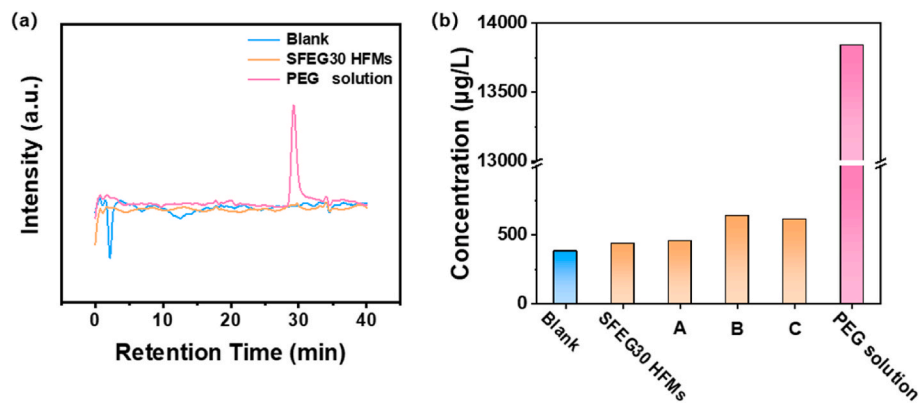
Fig. 6. (a) GPC traces of PEG solution and the dialysis water sample of SFEG30 HFMs. (b) TOC results of PEG solution, dialysis water sample of SFEG30 HFMs and the commercial membrane A, B, C.

after 4 h of dialysis of SFEG30 HFMs. It is suspected that organic matters such as the fragmentary PEG segments, acetone or *n*-propanol used as the swelling agent may be leached out during dialysis, however, the TOC results demonstrated that all organic solvents were completely removed during preparation and no other organics were generated during dialysis. Moreover, the TOC value of SFEG30 HFMs was smaller than that of commercial membrane A, B, and C. Therefore, SFEG30 HFMs could be considered as a "clean" membrane with little or no elution during hemodialysis. Considering the simplicity, effectiveness and additive-free characteristics of melt-spinning and selective swelling, SFEG30 HFMs are therefore a promising candidate for hemodialysis membranes with excellent selectivity and safety.

4. Conclusions

In this work, hemodialysis HFMs is prepared by melt spinning and selective swelling of block copolymer PSF-*b*-PEG for the first time. The SFEG30 HFMs prepared by selective swelling possess systematical structure with uniform pores and enhanced surface hydrophilicity. By systematically investigating the effect of block ratio and swelling conditions, SFEG30 HFMs prepared by swelling at 65 °C for 1 h is found to be most suitable in the precise separation of BSA and middle molecular toxins. SFEG30 HFMs show 99.9 % rejection to BSA, high clearance of lysozyme (69.2 %) and myoglobin (49.8 %). The PEG chains are attached to PSF through covalent bonds and migrate to membrane surfaces after swelling, leading to stable and long-standing hemocompatibility of the HFMs. SFEG30 HFMs exhibited good biocompatibility, *i.e.*, reduced BSA adsorption, negligible platelet adhesion and hemolysis rate and prolonged clotting time. More importantly, almost no elution of organic matters could be detected for SFEG30 HFMs after dialysis. Therefore, HFMs of block copolymers prepared by melt spinning and selective swelling is expected to be a promising candidate for hemodialysis membranes with excellent selectivity, biocompatibility and safety.

CRediT authorship contribution statement

Xiang Ying: Data curation, Investigation, Writing – original draft. **Shoutian Qiu:** Funding acquisition, Validation, Writing – review & editing. **Xiangyue Ye:** Investigation, Methodology. **Zhuo Li:** Investigation. **Jiemei Zhou:** Methodology, Validation. **Yong Wang:** Conceptualization, Funding acquisition, Supervision, Writing – review & editing.

Declaration of competing interest

The authors declare that they have no known competing financial interests or personal relationships that could have appeared to influence the work reported in this paper.

Data availability

Data will be made available on request.

Appendix A. Supplementary data

Supplementary data to this article can be found online at https://doi.org/10.1016/j.memsci.2024.122457.

References

[1] G.B.D.C.K.D. Collaboration, Global, regional, and national burden of chronic kidney disease, 1990-2017: a systematic analysis for the Global Burden of Disease Study 2017, Lancet 395 (2020) 709–733.
[2] J. Himmelfarb, R. Vanholder, R. Mehrotra, M. Tonelli, The current and future landscape of dialysis, Nat. Rev. Nephrol. 16 (2020) 573–585.
[3] P. Stenvinkel, D. Fouque, C. Wanner, Life/2020—the future of kidney disease, Nephrol. Dial. Transplant. 35 (2020) ii1–ii3.
[4] T. Yan, W. Peng, J. Lv, J. Wu, J. Chen, Hemodialysis or Peritoneal dialysis, which is better for patients with Delayed graft function? Kidney Blood Pressure Res 43 (2018) 1813–1821.
[5] M. Bernard, E. Jubeli, M.D. Pungente, N. Yagoubi, Biocompatibility of polymer-based biomaterials and medical devices - regulations, in vitro screening and risk-management, Biomater. Sci. 6 (2018) 2025–2053.
[6] N. Said, W.J. Lau, Y.C. Ho, S.K. Lim, M.N. Zainol Abidin, A.F. Ismail, A review of commercial Developments and recent Laboratory Research of dialyzers and membranes for hemodialysis application, Membranes 11 (2021) 767.
[7] A. Mollahosseini, A. Abdelrasoul, A. Shoker, A critical review of recent advances in hemodialysis membranes hemocompatibility and guidelines for future development, Mater. Chem. Phys. 248 (2020) 122911.
[8] Y. Torii, S. Yamada, M. Yajima, T. Sugata, Polymethylmethacrylate membrane dialyzer: Historic but modern, Blood Purif. (2022) 4–10.
[9] Q. Zhang, X. Lu, L. Zhao, Preparation of Polyvinylidene Fluoride (PVDF) hollow fiber hemodialysis membranes, Membranes 4 (2014) 81–95.
[10] O. ter Beek, D. Pavlenko, M. Suck, S. Helfrich, L. Bolhuis-Versteeg, D. Snisarenko, C. Causserand, P. Bacchin, P. Aimar, R. van Oerle, R. Wetzels, P. Verhezen, Y. Henskens, D. Stamatialis, New membranes based on polyethersulfone – SlipSkin™ polymer blends with low fouling and high blood compatibility, Sep. Purif. Technol. 225 (2019) 60–73.
[11] S.K. Verma, A. Modi, A.K. Singh, R. Teotia, J. Bellare, Improved hemodialysis with hemocompatible polyethersulfone hollow fiber membranes: in vitro performance, J. Biomed. Mater. Res., Part B 106 (2018) 1286–1298.
[12] H. Wang, J. Li, F. Liu, T. Li, Y. Zhong, H. Lin, J. He, Enhanced hemocompatibility of flat and hollow fiber membranes via a heparin free surface crosslinking strategy, React. Funct. Polym. 124 (2018) 104–114.
[13] S.U. Zaman, R. Saif Ur, M.K.U. Zaman, S. Rafiq, A. Arshad, M.S. Khurram, M. Irfan, S. Saqib, N. Muhammad, M. Irfan, F. Sharif, M.A. Bustam, M. Jamal, M.A. Khan, M. A. Waseem, A. Mukhtar, S. Wajeeh, Fabrication and performance evaluation of polymeric membrane using blood compatible hydroxyapatite for artificial kidney application, Artif. Organs 45 (2021) 1377–1390.

[14] T.R. Kim, M. Hadidi, S.P. Motevalian, T. Sunohara, A.L. Zydney, Effects of plasma proteins on the Transport and surface characteristics of polysulfone/polyethersulfone and asymmetric Cellulose Triacetate high flux dialyzers, Artif. Organs 42 (2018) 1070–1077.

[15] M. Weber, H. Steinle, S. Golombek, L. Hann, C. Schlensak, H.P. Wendel, M. Avci-Adali, Blood-contacting biomaterials: in vitro evaluation of the hemocompatibility, Front. Bioeng. Biotech. 6 (2018) 99.

[16] S. Tunc, M.F. Maitz, G. Steiner, L. Vazquez, M.T. Pham, R. Salzer, In situ conformational analysis of fibrinogen adsorbed on Si surfaces, Colloids Surf., B 42 (2005) 219–225.

[17] X. Song, H. Ji, W. Zhao, S. Sun, C. Zhao, Hemocompatibility enhancement of polyethersulfone membranes: Strategies and challenges, Adv. Membr. 1 (2021) 100013.

[18] W. Sun, W. Liu, Z. Wu, H. Chen, Chemical surface modification of polymeric biomaterials for biomedical applications, Macromol. Rapid Commun. 41 (2020) e1900430.

[19] L. Shan, Y. Sun, F. Shan, L. Li, Z.P. Xu, Recent advances in heparinization of polymeric membranes for enhanced continuous blood purification, J. Mater. Chem. B 8 (2020) 878–894.

[20] M.J. Han, S.T. Nam, Thermodynamic and rheological variation in polysulfone solution by PVP and its effect in the preparation of phase inversion membrane, J. Membr. Sci. 202 (2002) 55–61.

[21] J.D. Friedl, V. Nele, G. De Rosa, A. Bernkop-Schnürch, Bioinert, stealth or interactive: How surface Chemistry of nanocarriers Determines their fate in Vivo, Adv. Funct. Mater. 31 (2021) 2103347.

[22] A. Higuchi, K. Shirano, M. Harashima, B.O. Yoon, M.H.M. Hara, K. Imamura, Chemically modified polysulfone hollow fibers with vinylpyrrolidone having improved blood compatibility, J. Membr. Sci. 23 (2002) 2659–2666.

[23] A. Higuchi, K. Sugiyama, B.O. Yoon, M. Sakurai, M. Hara, M. Sumita, S. Sugawara, T. Shirai, Serum protein adsorption and platelet adhesion on pluronic-adsorbed polysulfone membranes, Biomaterials 24 (2003) 3235–3245.

[24] B. Chakrabarty, A.K. Ghoshal, M.K. Purkait, Preparation, characterization and performance studies of polysulfone membranes using PVP as an additive, J. Membr. Sci. 315 (2008) 36–47.

[25] L.-S. Wan, Z.-K. Xu, Z.-G. Wang, Leaching of PVP from polyacrylonitrile/PVP blending membranes: a comparative study of asymmetric and dense membranes, J. Polym. Sci., Part B: Polym. Phys. 44 (2006) 1490–1498.

[26] A. Taubert, A. Napoli, W. Meier, Self-assembly of reactive amphiphilic block copolymers as mimetics for biological membranes, Curr. Opin. Chem. Biol. 8 (2004) 598–603.

[27] F. Ran, S. Nie, W. Zhao, J. Li, B. Su, S. Sun, C. Zhao, Biocompatibility of modified polyethersulfone membranes by blending an amphiphilic triblock co-polymer of poly(vinyl pyrrolidone)-b-poly(methyl methacrylate)-b-poly(vinyl pyrrolidone), Acta Biomater. 7 (2011) 3370–3381.

[28] H. Song, F. Ran, H. Fan, X. Niu, L. Kang, C. Zhao, Hemocompatibility and ultrafiltration performance of surface-functionalized polyethersulfone membrane by blending comb-like amphiphilic block copolymer, J. Membr. Sci. 471 (2014) 319–327.

[29] D. Zhong, Z. Wang, J. Zhou, Y. Wang, Additive-free preparation of hemodialysis membranes from block copolymers of polysulfone and polyethylene glycol, J. Membr. Sci. 618 (2021) 118690.

[30] G. Donati, M. Cappuccilli, C. Donadei, M. Righini, A. Scrivo, L. Gasperoni, F. Zappulo, G. La Manna, Toxin removal and Inflammatory state Modulation during online Hemodiafiltration using two different dialyzers (TRIAD2 study), Methods Protoc 4 (2021) 26.

[31] D. Zhong, J. Zhou, Y. Wang, Hollow-fiber membranes of block copolymers by melt spinning and selective swelling, J. Membr. Sci. 632 (2021) 119374.

[32] J. Calvo, R. Peinador, P. Prádanos, L. Palacio, A. Bottino, G. Capannelli, A. Hernández, Liquid–liquid displacement porometry to estimate the molecular weight cut-off of ultrafiltration membranes, Desalination 268 (2011) 174–181.

[33] P.M. Aimar, S.M. Sanchez, A contribution to the translation of retention curves into pore size distributions for sieving membranes, J. Membr. Sci. 54 (1990) 321–338.

[34] A. Boschetti-de-Fierro, M. Voigt, M. Storr, B. Krause, Extended characterization of a new class of membranes for blood purification: the high cut-off membranes, Int. J. Artif. Organs 36 (2013) 455–463.

[35] J. Zhou, Y. Wang, Selective swelling of block copolymers: an Upscalable Greener process to ultrafiltration membranes? Macromolecules 53 (2019) 5–17.

[36] J. Wang, H. Guan, Q. Liang, M. Ding, Construction of copper (II) affinity- DTPA functionalized magnetic composite for efficient adsorption and specific separation of bovine hemoglobin from bovine serum, Composites, Part B 198 (2020) 108248.

[37] G.-d. Zhu, Y.-r. Ying, X. Li, Y. Liu, C.-y. Yang, Z. Yi, C.-j. Gao, Isoporous membranes with sub-10 nm pores prepared from supramolecular interaction facilitated block copolymer assembly and application for protein separation, J. Membr. Sci. 566 (2018) 25–34.

[38] Y. Huang, P. Yang, F. Yang, C. Chang, Self-supported nanoporous lysozyme/nanocellulose membranes for multifunctional wastewater purification, J. Membr. Sci. 635 (2021) 119537.

[39] J. Zhou, C. Zhang, C. Shen, Y. Wang, Synthesis of poly(2-dimethylaminoethyl methacrylate)-block- poly(styrene-alt-N-phenylmaleimide) and its thermo-tolerant nanoporous films prepared by selective swelling, Polymer 164 (2019) 126–133.

[40] C. Ronco, W.R. Clark, Haemodialysis membranes, Nat. Rev. Nephrol. 14 (2018) 394–410.

[41] L.C. Xu, J.W. Bauer, C.A. Siedlecki, Proteins, platelets, and blood coagulation at biomaterial interfaces, Colloids Surf., B 124 (2014) 49–68.

[42] Z. Wang, R. Liu, H. Yang, Y. Wang, Nanoporous polysulfones with in situ PEGylated surfaces by a simple swelling strategy using paired solvents, Chem. Commun. 53 (2017) 9105–9108.

[43] S. Schottler, G. Becker, S. Winzen, T. Steinbach, K. Mohr, K. Landfester, V. Mailander, F.R. Wurm, Protein adsorption is required for stealth effect of poly (ethylene glycol)- and poly(phosphoester)-coated nanocarriers, Nat. Nanotechnol. 11 (2016) 372–377.

[44] W.B. Tsai, J.M. Grunkemeier, C.D. McFarland, T.A. Horbett, Platelet adhesion to polystyrene-based surfaces preadsorbed with plasmas selectively depleted in fibrinogen, fibronectin, vitronectin, or von Willebrand's factor, J. Biomed. Mater. Res. 60 (2002) 348–359.

[45] R. Tzoneva, M. Heuchel, T. Groth, G. Altankov, W. Albrecht, D. Paul, Fibrinogen adsorption and platelet interactions on polymer membranes, J. Biomater. Sci. Polym. Ed. 13 (2002) 1033–1050.

[46] J. Kuchinka, C. Willems, D.V. Telyshev, T. Groth, Control of blood coagulation by hemocompatible material surfaces-A review, Bioengineering 8 (2021) 215.

[47] B. Kalaska, K. Kaminski, J. Miklosz, K. Nakai, S.I. Yusa, D. Pawlak, M. Nowakowska, A. Mogielnicki, K. Szczubialka, Anticoagulant properties of poly (sodium 2-(acrylamido)-2-methylpropanesulfonate)-Based Di- and triblock polymers, Biomacromolecules 19 (2018) 3104–3118.